



ARTICLE

Secrecy Outage Probability for Two-Way Integrated Satellite Unmanned Aerial Vehicle Relay Networks with Hardware Impairments

Xiaoting Ren¹ and Kefeng Guo^{2,*}

¹College of Public Management, China University of Mining and Technology, Xuzhou, 221116, China

²School of Space Information, Space Engineering University, Beijing, 101407, China

*Corresponding Author: Kefeng Guo. Email: guokefeng.cool@163.com

Received: 09 June 2022 Accepted: 14 July 2022

ABSTRACT

In this paper, we investigate the secrecy outage performance for the two-way integrated satellite unmanned aerial vehicle relay networks with hardware impairments. Particularly, the closed-form expression for the secrecy outage probability is obtained. Moreover, to get more information on the secrecy outage probability in a high signal-to-noise regime, the asymptotic analysis along with the secrecy diversity order and secrecy coding gain for the secrecy outage probability are also further obtained, which presents a fast method to evaluate the impact of system parameters and hardware impairments on the considered network. Finally, Monte Carlo simulation results are provided to show the efficiency of the theoretical analysis.

KEYWORDS

Integrated satellite unmanned aerial vehicle relay networks; two-way unmanned aerial vehicle relay; hardware impairments; secrecy outage probability (SOP); asymptotic SOP

1 Introduction

It is reported that satellite communication (SatCom) is considered to be a promising way for the sixth generation (6G) and beyond next generation (BNG) wireless communication system for its special characters, such as the wide coverage and particular services [1–5]. Owing to similar reasons, it can make up for the shortage of unmanned aerial vehicle (UAV) networks along with the high data transmission and wide coverage. Based on this foundation, to both utilize the advantage of the SatCom and UAV networks, the framework for the integrated satellite UAV relay network (ISUAVRN) appears, which is considered the major part of the future wireless communication networks [6,7]. Besides, owing to the transmission beam's wide coverage, many users or relays existed in one beam [7–11]. In [7], a selection scheme based on the threshold was provided to keep the balance between the system performance and system complexity for the considered network. Furthermore, the outage probability (OP) was studied. In [8], one partial selection scheme was utilized to enhance the system performance for the considered networks. In [9], the authors studied the OP for the cognitive networks, which combined the satellite and the terrestrial networks. In [10], the OP was researched for the considered networks along with the secondary network selection scheme under the cognitive technology. In [11],



the authors gave a terrestrial and user scheduling scheme based on the maximal performance for the ISUAVRN in the presence of many terrestrial relays and many users. In [12], the ergodic capacity for the ISUAVRN with a selection scheme and multiple terrestrial relays was researched. In [13], the OP was investigated for the ISUAVRN with multiple users and an opportunistic user scheduling scheme. To enhance the spectrum efficiency and time utilization, a two-way relay technique is proposed for the ISUAVRN [14]. In [15], the OP was researched for the ISUAVRN with hardware impairments (HIs) and the two-way terrestrial relay. In [16], the OP was analyzed for the ISUAVRN in the presence of many two-way terrestrial relays and a partial selection scheme. In [17], the OP was investigated for the considered ISUAVRN with multiple terrestrial relays and an opportunistic selection scheme under the non-orthogonal multiple access scenario. However, due to the inherent characters of wireless communications particularly for the SatCom, the secrecy issue has been regarded as the major point for the SatCom [18]. The physical layer security (PLS) is considered as the hopeful method to investigate the difference between the eavesdroppers' and legitimate channels, which is a popular research issue over recent years [19,20]. In [19], a proposed beamforming (BF) scheme was utilized for the cognitive ISUAVRN to enhance the secrecy performance. In [21], the authors researched the secrecy-energy efficient hybrid BF scheme for the ISUAVRN. In [22], the non-ideal channel state information (CSI) and cognitive technology were both investigated for the secrecy ISUAVRN along with secrecy performance. In practical systems, all nodes are not often ideal, which means they always suffer the I/Q imbalance, phase noise, and amplifier non-linearities [23–25], which results in the HIs in the transmission nodes. In [26], all the HIs issues are concluded, which leads to a general HIs model, widely utilized for many former works [27–31]. Above all, to the authors' best effort, the investigation for the effects of two-way terrestrial relays on the secrecy ISUAVRN with HIs is still not published, which motivates our paper.

From the former discussions, by considering the two-way UAV relay and an eavesdropper into our sight, we investigate the secrecy performance for the considered network. The contributions of this paper are presented in the following:

- By utilizing the two-way UAV relay and an eavesdropper into consideration, the framework for the secrecy ISUAVRN is founded. Besides, the decode-and-forward (DF) mode is used in the UAV to help the source to transmit the signals. Due to the heavy fading and other obstacle reasons, no direct link is assumed for the legitimate transmission link for the two sources. In addition, all the nodes are assumed to suffer from the HIs.
- Based on the considered system model, the detailed analysis for the secrecy outage probability (SOP) is obtained, which gives the easy method to investigate the SOP. Besides, these theoretical results can direct the engineering guide.
- To derive the further results of the system parameters on the SOP for the system, the asymptotic behaviors for the SOP are derived, which provide the secrecy diversity and order secrecy coding gain.

The remaining of this paper is shown in the following. A detailed illustration for the considered system is given in Section 2. The analysis for the secrecy OP is derived in Section 3. Some computer simulations namely Monte Carlo (MC) results are given in Section 4 to show the efficiency of the analytical results. The conclusion of the work is provided in Section 5.

Notations: $|\cdot|$ represents the absolute value of a complex scalar. $E[\cdot]$ is the expectation operator, $\mathcal{CN}(\mathbf{a}, \mathbf{B})$ denotes the complex Gaussian distribution of a random vector \mathbf{a} and covariance matrix \mathbf{B} . $F_y(\cdot)$ and $f_y(\cdot)$ represent the cumulative distribution function (CDF) and probability density function (PDF) of the random variable y , respectively. The abbreviations are given in Table 1.

Table 1: Abbreviations

AS	Average shadowing
AWGN	Additive white Gaussian noise
BF	Beamforming
BNG	Beyond next generation
CDF	Cumulative distribution function
CSI	Channel state information
DF	Decode-and-forward
FHS	Frequency heavy shadowing
FSL	Free space loss
GEO	Geosynchronous Earth orbit
HI	Hardware impairments
i.i.d	Independent and identically distribution
ILS	Infrequent light shadowing
ISUAVRNs	Integrated satellite UAV relay networks
LMS	Land mobile satellite
LOS	Line of sight
MC	Monte Carlo
OP	Outage probability
PLS	Physical layer security
PDF	Probability density function
SatCom	Satellite communication
SINR	Signal-to-interference-plus-noise ratio
SNR	Signal-to-noise ratio
SOP	Secrecy outage probability
SR	Shadowed-Rician
TDMA	Time division multiple access
UAV	Unmanned aerial vehicle

2 System Model

As plotted in Fig. 1, we consider an ISUAVRN with HIs in this paper, which contains a satellite source S_1 , one terrestrial user S_2 , a two-way UAV R and an eavesdropper E . The two-way UAV R works in DF mode. The whole nodes are considered to have one antenna and suffer from the HIs¹. At the same time, an eavesdropper UAV E^2 exist in the similar transmission beam with R and wants to overhear the transmission signals from S_1 , S_2 and R . Due to the high building and the other reasons, no direct transmission link is considered between the S_1 and S_2 , which results in that the signal can only be transmitted by R^3 .

¹ We should know that, during this paper, only one antenna is assumed, however the derived results are still fit for the case with many antennas.

² Although this paper just considers one eavesdropper, the derived results are still fit for the model with multiple eavesdroppers. Besides, the model with multiple eavesdroppers will be investigated in our near future.

³ Owing to some reasons, direct transmission link between two sources is not available.

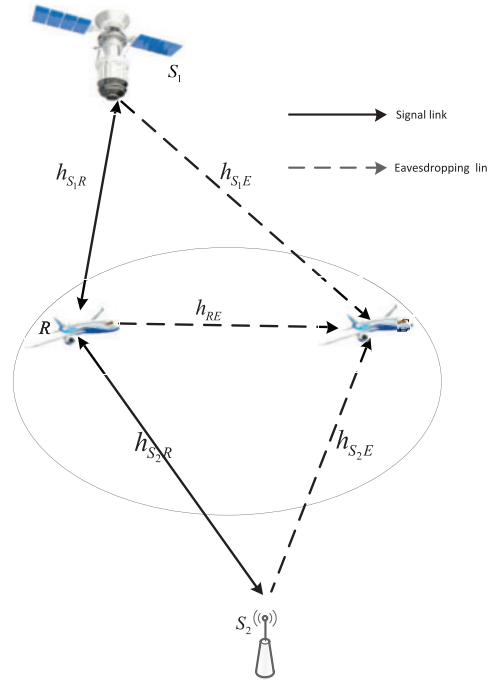


Figure 1: The system model description

It will use two time slots for the whole transmission. During the first time slot, S_1 and S_2 send its own symbols in the same time slot, i.e., $s_1(t)$ with $E[|s_1(t)|^2] = 1$ and $s_2(t)$ with $E[|s_2(t)|^2] = 1$ to R , respectively. So, the obtained signal at R is shown as

$$y_R(t) = \sqrt{P_{S_1}} h_{S_1R} [s_1(t) + \eta_1(t)] + \sqrt{P_{S_2}} h_{S_2R} [s_2(t) + \eta_2(t)] + n_R(t), \quad (1)$$

where P_{S_1} represents the transmitted power of S_1 , P_{S_2} represents the power for the S_2 . h_{S_1R} denotes the channel coefficient for the $S_1 \rightarrow R$ transmission link with modeling as the shadowed-Rician (SR) fading. h_{S_2R} represents the channel coefficient for the $S_2 \rightarrow R$ link with Rayleigh shadowing. As presented before, the transmission nodes suffer from the HIs; $\eta_1(t)$ and $\eta_2(t)$ denote the distortion noise due to HIs at S_1 and S_2 , respectively, which are shown as $\eta_1(t) \sim \mathcal{CN}(0, k_1^2)$ and $\eta_2(t) \sim \mathcal{CN}(0, k_2^2)$. k_1 and k_2 represent the HIs level at the S_1 and S_2 , respectively [2]. $n_R(t)$ represents the additive white Gaussian noise (AWGN) at R with modeling as $n_R(t) \sim \mathcal{CN}(0, \delta_R^2)$.

Since E and R are located in the same transmission beam, the overhear signal at E in the first time slot is shown as

$$y_{S_pE}(t) = \sqrt{P_{S_p}} h_{S_pE} [s_p(t) + \eta_p(t)] + n_E(t), p \in \{1, 2\}, \quad (2)$$

where $y_{S_pE}(t)$ represents the signal received at E from the p -th source, P_{S_p} denotes the p -th source's power, h_{S_pE} is the channel fading between the p -th source and E with SR and Rayleigh fading, respectively. $n_E(t)$ denotes the AWGN at E with modeling as $n_E(t) \sim \mathcal{CN}(0, \delta_E^2)$.

In the second time slot, owing to the utilized DF protocol, the UAV relay will use some techniques to decode the signals received and then re-transmit the re-encoded signal to S_p , respectively. Since S_p

knows their own signals, and they can know its signals and delete the self-interference, the obtained signal at S_p is shown as

$$y_{RS_p}(t) = \sqrt{P_R} h_{S_p R} [s_p(t) + \eta_R(t)] + n_{S_p}(t), \tag{3}$$

where P_R represents the R 's power, $\eta_R(t)$ is the distortion noise which comes from the HIs with $\eta_R(t) \sim \mathcal{CN}(0, k_R^2)$, k_R is the impairments' level at R [2]. $n_{S_p}(t)$ denotes the AWGN at S_p which has the presentation as $n_{S_p}(t) \sim \mathcal{CN}(0, \delta_{S_p}^2)$.

As the same assumption, R and E are located in the similar transmission beam. Thus, the obtained signal at E in the second time slot is represented as

$$y_{RE}(t) = \sqrt{P_R} h_{RE} [s_p(t) + \eta_R(t)] + n_E(t), \tag{4}$$

where h_{RE} represents the channel coefficient between E and R , which is shown as Rayleigh fading.

By utilizing Eqs. (1) and (3), the obtained signal-to-interference-plus-noise ratio (SINR) at R from the p -th source is obtained as

$$\gamma_{S_1 R} = \frac{P_{S_1} |h_{S_1 R}|^2}{P_{S_1} |h_{S_1 R}|^2 k_1^2 + P_{S_2} |h_{S_2 R}|^2 (1 + k_2^2) + \delta_R^2} \tag{5}$$

$$= \frac{\gamma_{1S_1 R}}{\gamma_{1S_1 R} k_1^2 + \gamma_{2S_2 R} (1 + k_2^2) + 1},$$

$$\gamma_{S_2 R} = \frac{\gamma_{2S_2 R}}{\gamma_{2S_2 R} k_2^2 + \gamma_{1S_1 R} (1 + k_1^2) + 1}, \tag{6}$$

where $\gamma_{1S_1 R} = P_{S_1} |h_{S_1 R}|^2 / \delta_R^2$ and $\gamma_{2S_2 R} = P_{S_2} |h_{S_2 R}|^2 / \delta_R^2$.

The derived signal-to-noise ratio (SNR) at S_p is given as

$$\gamma_{RS_p} = \frac{P_R |h_{RS_p}|^2}{P_R |h_{RS_p}|^2 k_R^2 + \delta_{S_p}^2} = \frac{\gamma_{RRS_p}}{\gamma_{RRS_p} k_R^2 + 1}, \tag{7}$$

where $\gamma_{RRS_p} = \frac{P_R |h_{RS_p}|^2}{\delta_{S_p}^2}$.

With the help of Eqs. (2) and (4), the obtained SNR at E is, respectively, obtained as

$$\gamma_{S_p E} = \frac{P_{S_p} |h_{S_p E}|^2}{P_{S_p} |h_{S_p E}|^2 k_p^2 + \delta_E^2} = \frac{\gamma_{pS_p E}}{\gamma_{pS_p E} k_p^2 + 1}, \tag{8}$$

$$\gamma_{RE} = \frac{P_R |h_{RE}|^2}{P_R |h_{RE}|^2 k_R^2 + \delta_E^2} = \frac{\gamma_{RRE}}{\gamma_{RRE} k_R^2 + 1}. \tag{9}$$

where $\gamma_{pS_p E} = \frac{P_{S_p} |h_{S_p E}|^2}{\delta_E^2}$ and $\gamma_{RRE} = \frac{P_R |h_{RE}|^2}{\delta_E^2}$.

According to [32], the capacity for secrecy performance has the definition which is shown as the difference between the capacity of the legitimate users' channel and the eavesdroppers' channel. By

utilizing Eqs. (5)–(9), the secrecy capacity for the considered network is represented as

$$C_S = \min(C_{S_1}, C_{S_2}), \quad (10)$$

where $C_{S_1} = \min(C_{S_{11}}, C_{S_{22}})$, $C_{S_2} = \min(C_{S_{12}}, C_{S_{21}})$, $C_{S_{11}} = [\log_2(1 + \gamma_{S_1R}) - \log_2(1 + \gamma_{S_1E})]^+$, $C_{S_{22}} = [\log_2(1 + \gamma_{RS_2}) - \log_2(1 + \gamma_{RE})]^+$, $C_{S_{12}} = [\log_2(1 + \gamma_{S_2R}) - \log_2(1 + \gamma_{S_2E})]^+$ and $C_{S_{21}} = [\log_2(1 + \gamma_{RS_1}) - \log_2(1 + \gamma_{RE})]^+$ with $[x]^+ \triangleq \max[x, 0]$.

3 Secrecy System Performance

The detailed analysis for the SOP will be obtained in this part. At first, the channel model for the transmission link is presented.

3.1 The Channel Model

3.1.1 The Terrestrial Transmission Link

The channel model for the terrestrial transmission link is modeled as independent and identically distribution (i.i.d) Rayleigh fading. From [33], the PDF and CDF of γ_X , $X \in \{2S_2R, RRE, RRS_2, 2S_2E\}$, are respectively derived as

$$f_{\gamma_X}(x) = \frac{1}{\bar{\gamma}_X} e^{-\frac{x}{\bar{\gamma}_X}} \quad (11)$$

and

$$F_{\gamma_X}(x) = 1 - e^{-\frac{x}{\bar{\gamma}_X}}, \quad (12)$$

where $\bar{\gamma}_X$ represents the average channel gain.

3.1.2 The Satellite Transmission Link

The geosynchronous Earth orbit (GEO) satellite is taken for the analysis. In addition, we also consider the satellite having multiple beams for the considered system model. Particularly, time division multiple access (TDMA) [34] scheme is utilized in the considered model, which means that only one UAV R is suitable to forward the information signal at the next time slot.

The channel coefficient h_V , $V \in \{1S_1R, 1S_1E, RRS_1\}$ between the downlink on-board beam satellite and UAV is presented as

$$h_V = C_V f_V, \quad (13)$$

where f_V represents the random SR coefficient, C_V represents the effects of the antenna pattern and free space loss (FSL), which can be re-given by

$$C_V = \frac{\lambda \sqrt{G_V G_{Re}}}{4\pi \sqrt{d^2 + d_0^2}}, \quad (14)$$

where λ denotes the frequency carrier's wavelength, d is the length between UAV/eavesdropper and the satellite. $d_0 \approx 35786$ km represents the antenna gain for UAV/eavesdropper and G_{Re} represents the satellite's on-board beam gain.

With help of [35], G_{Re} can be written as

$$G_{Re} (dB) \simeq \begin{cases} \bar{G}_{\max}, & \text{for } 0^\circ < \vartheta < 1^\circ \\ 32 - 25 \log \vartheta, & \text{for } 1^\circ < \vartheta < 48^\circ \\ -10, & \text{for } 48^\circ < \vartheta \leq 180^\circ, \end{cases} \quad (15)$$

where \bar{G}_{\max} represents the maximum beam gain at the boresight, and ϑ denotes the angle of the off-boresight. Recalling G_V , by considering θ_k as the angle between UAV/eavesdropper position and the satellite. In addition, $\bar{\theta}_k$ represents the 3 dB angle of satellite beam. The antenna gain can be shown as [2,35]

$$G_V \simeq G_{\max} \left(\frac{K_1(u_k)}{2u_k} + 36 \frac{K_3(u_k)}{u_k^3} \right), \quad (16)$$

where G_{\max} presents the maximal beam gain, $u_k = 2.07123 \sin \theta_k / \sin \bar{\theta}_k$, K_3 and K_1 denote the 1st-kind Bessel function of order 3 and 1, respectively. In order to gain best performance, thus, $\theta_k \rightarrow 0$ is set, which leads to $G_V \approx G_{\max}$. Relying on this consideration, we derive $h_V = C_V^{\max} f_V$ with $C_V^{\max} = \frac{\lambda \sqrt{G_{\max} G_{Re}}}{4\pi \sqrt{d^2 + d_0^2}}$.

For f_V , a famous SR model was proposed in [36], which fits land mobile satellite (LMS) communication [2]. By utilizing [36], the channel coefficient f_V can be re-given as $f_V = \bar{f}_V + \tilde{f}_V$, where the scattering components \tilde{f}_V follows the i.i.d Rayleigh fading distribution while \bar{f}_V represents the element of line of sight (LOS) component which obeys i.i.d Nakagami- m distribution⁴.

With the help of [8], the PDF for $\gamma_V = \bar{\gamma}_V C_V^{\max} |f_V|^2$ is given by

$$f_{\gamma_V}(x) = \sum_{k_1=0}^{m_V-1} \frac{\alpha_V (1 - m_V)_{k_1} (-\delta_V)^{k_1} x^{k_1}}{(k_1!)^2 \bar{\gamma}_V^{k_1+1} \exp(\Delta_V x)}, \quad (17)$$

where $\Delta_V = \frac{\beta_V - \delta_V}{\bar{\gamma}_V}$, $\alpha_V = \left(\frac{2b_V m_V}{2b_V m_V + \Omega_V} \right)^{m_V} / (2b_V)$, $\beta_V = 1 / (2b_V)$ and $\delta_V = \frac{\Omega_V}{2b_V (2b_V m_V + \Omega_V)}$ with $m_V \geq 0$ regarding as the fading severity parameter with integer being. $2b_V$ represents the average power of the multi-path component. Ω_V represents the LOS component's average power. $\bar{\gamma}_V$ represents the transmission link's average SNR.

Relying on Eq. (17) and utilizing [11], the CDF of γ_V is re-derived as

$$F_{\gamma_V}(x) = 1 - \sum_{k_1=0}^{m_V-1} \sum_{t=0}^{k_1} \frac{\alpha_V (1 - m_V)_{k_1} (-\delta_V)^{k_1} x^t}{k_1! t! \bar{\gamma}_V^{k_1+1} \Delta_V^{k_1-t+1} \exp(\Delta_V x)}. \quad (18)$$

3.1.3 Secrecy Outage Probability

From [18], the SOP defined as

$$\begin{aligned} P_{out}(\gamma_0) &= \Pr(C_S \leq C_0) = \Pr[\min(C_{S_1}, C_{S_2}) \leq C_0] \\ &= \Pr(C_{S_1} \leq C_0) + \Pr(C_{S_2} \leq C_0) - \Pr(C_{S_1} \leq C_0) \Pr(C_{S_2} \leq C_0), \end{aligned} \quad (19)$$

where $C_0 = \log_2(1 + \gamma_0)$ with γ_0 defined as the target threshold.

⁴It should be mentioned that, the SR channel is a famous channel model [8,10], which comes from the practical estimation date [37,38].

For $S_1 \rightarrow S_2$ transmission link:

$$\Pr(C_{S_1} \leq C_0) = \Pr(C_{S_{11}} \leq C_0) + \Pr(C_{S_{22}} \leq C_0) - \Pr(C_{S_{11}} \leq C_0) \Pr(C_{S_{22}} \leq C_0), \tag{20}$$

For $S_2 \rightarrow S_1$ transmission link:

$$\Pr(C_{S_2} \leq C_0) = \Pr(C_{S_{12}} \leq C_0) + \Pr(C_{S_{21}} \leq C_0) - \Pr(C_{S_{12}} \leq C_0) \Pr(C_{S_{21}} \leq C_0). \tag{21}$$

Firstly, with the help of $C_{S_{11}} = [\log_2(1 + \gamma_{S_{1R}}) - \log_2(1 + \gamma_{S_{1E}})]^+$, $\Pr(C_{S_{11}} \leq C_0)$ can be obtained as

$$\Pr(C_{S_{11}} < C_0) = \Pr[\log_2(1 + \gamma_{S_{1R}}) - \log_2(1 + \gamma_{S_{1E}}) < \log_2(1 + \gamma_0)] = \Pr[\gamma_{S_{1R}} < \gamma_0 + (\gamma_0 + 1) \gamma_{S_{1E}}]. \tag{22}$$

From Eq. (22), the first consideration is to obtain the CDF for $\gamma_{S_{1R}}$ and PDF for $\gamma_{S_{1E}}$. The PDF for $\gamma_{1S_{1E}}$ has been give in Eq. (17) with $V = 1S_1E$, thus utilizing the Eqs. (8) and (17), the PDF for $\gamma_{S_{1E}}$ can be re-written as

$$f_{\gamma_{S_{1E}}}(x) = \frac{1}{(1 - k_1^2 x)^2} \sum_{k_{11}=0}^{m_{S_{1E}}-1} \frac{\alpha_{S_{1E}} (1 - m_{S_{1E}})_{k_{11}} (-\delta_{S_{1E}})^{k_{11}}}{(k_{11}!)^2 \bar{\gamma}_{S_{1E}}^{k_{11}+1}} \left(\frac{x}{1 - k_1^2 x}\right)^{k_{11}} \exp\left(\frac{-\Delta_{S_{1E}} x}{1 - k_1^2 x}\right). \tag{23}$$

Then by utilizing Eq. (5), the CDF for $\gamma_{S_{1R}}$ is re-written as

$$F_{\gamma_{S_{1R}}}(x) = \Pr(\gamma_{S_{1R}} \leq x) = \Pr\left(\frac{\gamma_{1S_{1R}}}{\gamma_{1S_{1R}} k_1^2 + \gamma_{2S_{2R}} (1 + k_2^2) + 1} \leq x\right) = \Pr\left\{\gamma_{1S_{1R}} \leq \left[\frac{\gamma_{2S_{2R}} (1 + k_2^2) x}{1 - k_1^2 x} + \frac{x}{1 - k_1^2 x}\right]\right\}. \tag{24}$$

With the help of Eq. (17) with $V = 1S_1R$ and Eq. (11) with $X = 2S_2R$, then we can get

$$F_{S_{1R}}(x) = 1 - \sum_{k_1=0}^{m_{1S_{1R}}-1} \sum_{t=0}^{k_1} \frac{\alpha_{1S_{1R}} (1 - m_{1S_{1R}})_{k_1} (-\delta_{1S_{1R}})^{k_1}}{k_1! t! \bar{\gamma}_{1S_{1R}}^{k_1+1} \Delta_{1S_{1R}}^{k_1-t+1} \bar{\gamma}_{2S_{2R}}} \times \int_0^\infty \underbrace{\left(\frac{y(1 + k_2^2)x}{1 - k_1^2 x} + \frac{x}{1 - k_1^2 x}\right)^t \exp\left[-\Delta_{1S_{1R}} \left(\frac{y(1 + k_2^2)x}{1 - k_1^2 x} + \frac{x}{1 - k_1^2 x}\right) - \frac{y}{\bar{\gamma}_{2S_{2R}}}\right]}_{I_1} dy. \tag{25}$$

Then, after some mathematic steps, I_1 is re-given by

$$I_1 = \exp\left(-\frac{\Delta_{1S_{1R}} x}{1 - k_1^2 x}\right) \sum_{p=0}^t \binom{t}{p} \left(\frac{x}{1 - k_1^2 x}\right)^t (1 + k_2^2)^p \times \underbrace{\int_0^\infty y^p \exp\left(-\frac{\Delta_{1S_{1R}} (1 + k_2^2) xy}{1 - k_1^2 x} - \frac{y}{\bar{\gamma}_{2S_{2R}}}\right) dy}_{I_2}. \tag{26}$$

Next, with the help of [39], I_2 can be obtained as

$$I_2 = p! \left(\frac{\Delta_{1S_1R} (1 + k_2^2) x}{1 - k_1^2 x} + \frac{1}{\bar{\gamma}_{2S_2R}} \right)^{-p-1}. \tag{27}$$

Then, recalling Eq. (22), Eq. (22) can be re-written as

$$\Pr(C_{S_{11}} < C_0) = \Pr[\gamma_{S_1R} < \gamma_0 + (\gamma_0 + 1) \gamma_{S_1E}] = \int_0^\infty F_{\gamma_{S_1R}}[\gamma_0 + (\gamma_0 + 1) y] f_{\gamma_{S_1E}}(y) dy. \tag{28}$$

Then, it should be mentioned that in Eqs. (23) and (24), y should be satisfied with the following condition, which is $y \leq 1/k_1^2$ and $y < \frac{1/k_1^2 - \gamma_0}{\gamma_0 + 1}$. Next, by submitting Eqs. (23) and (24) into Eq. (28), Eq. (28) is rewritten as

$$\Pr(C_{S_{11}} < C_0) = \int_0^{H_1} F_{\gamma_{S_1R}}[\gamma_0 + (\gamma_0 + 1) y] f_{\gamma_{S_1E}}(y) dy + \int_{H_1}^{H^1} f_{\gamma_{S_1E}}(y) dy, \tag{29}$$

where $H_1 = \min\left(\frac{1/k_1^2 - \gamma_0}{\gamma_0 + 1}, \frac{1}{k_1^2}\right)$ and $H^1 = \max\left(\frac{1/k_1^2 - \gamma_0}{\gamma_0 + 1}, \frac{1}{k_1^2}\right)$.

However, try the authors' best efforts, it is too hard to obtain the closed-form expression of Eq. (29), then by utilizing [35] and utilizing the Gaussian-Chebyshev quadrature [40], by inserting Eqs. (24) and (23) into Eq. (29), it can be derived as

$$\begin{aligned} \Pr(C_{S_{11}} < C_0) &= 1 - \int_0^{H_1} \left\{ 1 - F_{\gamma_{S_1R}}[\gamma_0 + (\gamma_0 + 1) y] \right\} f_{\gamma_{S_1E}}(y) dy \\ &= 1 - \sum_{k_1=0}^{m_{1S_1R}-1} \sum_{t=0}^{k_1} \sum_{k_{11}=0}^{m_{S_1E}-1} \sum_{p=0}^t \binom{t}{p} \\ &\quad \frac{(1 + k_2^2)^p p! \alpha_{S_1E} (1 - m_{S_1E})_{k_{11}} (-\delta_{S_1E})^{k_{11}} \alpha_{1S_1R} (1 - m_{1S_1R})_{k_1} (-\delta_{1S_1R})^{k_1}}{(k_{11}!)^2 \bar{\gamma}_{S_1E}^{-k_{11}+1} k_1! t! \bar{\gamma}_{1S_1R}^{-k_1+1} \Delta_{1S_1R}^{k_1-t+1} \bar{\gamma}_{2S_2R}} \times \frac{H_1}{2} \sum_{l=1}^{N_1} w_l H_l(y_l), \end{aligned} \tag{30}$$

where

$$\begin{aligned} H_1(y) &= \left(\frac{[\gamma_0 + (\gamma_0 + 1) y]}{1 - k_1^2 [\gamma_0 + (\gamma_0 + 1) y]} \right)^t \exp \left\{ -\frac{\Delta_{1S_1R} [\gamma_0 + (\gamma_0 + 1) y]}{1 - k_1^2 [\gamma_0 + (\gamma_0 + 1) y]} - \frac{\Delta_{S_1E} y}{1 - k_1^2 y} \right\} \\ &\times \left(\frac{\Delta_{1S_1R} (1 + k_2^2) [\gamma_0 + (\gamma_0 + 1) y]}{1 - k_1^2 [\gamma_0 + (\gamma_0 + 1) y]} + \frac{1}{\bar{\gamma}_{2S_2R}} \right)^{-p-1} \frac{y^{k_{11}}}{(1 - k_1^2 y)^{k_{11}+2}}, \end{aligned}$$

and N_1 being the number of the terms, $y_l = \frac{H_1}{2} (x_l + 1)$ denotes the l -th zero of Legendre polynomials, w_l represents the Gaussian weight, which can be found in [40].

By utilizing the similar ways, the closed-form expressions for the $\Pr(C_{S_{22}} < C_0)$, $\Pr(C_{S_{12}} < C_0)$, and $\Pr(C_{S_{21}} < C_0)$ are respectively obtained as

$$\Pr(C_{S_{22}} < C_0) = 1 - \frac{H_2}{2\bar{\gamma}_{RRE}} \sum_{v=1}^{N_2} \varpi_v H_2(y_v), \tag{31}$$

where

$$H_2(y) = \frac{1}{(1 - k_R^2 y)^2} \exp \left\{ -\frac{\gamma_0 + (\gamma_0 + 1) y}{\bar{\gamma}_{RRS_2} \{1 - k_R^2 [\gamma_0 + (\gamma_0 + 1) y]\}} - \frac{y}{\bar{\gamma}_{RRE} (1 - k_R^2 y)} \right\}$$

and N_2 being the number of the terms, $y_v = \frac{H_2}{2} (x_v + 1)$ represents the v -th zero of Legendre polynomials, ϖ_v is the Gaussian weight, which is shown in [40], and $H_2 = \min\left(\frac{1/k_R^2 - \gamma_0}{\gamma_0 + 1}, \frac{1}{k_R^2}\right)$.

$$\Pr(C_{S_{12}} < C_0) = 1 - \frac{H_3}{2} \sum_{k_{12}=0}^{m_{1S_1R}-1} \frac{\alpha_{1S_1R} (1 - m_{1S_1R})_{k_{12}} (-\delta_{1S_1R})^{k_{12}}}{k_{12}! \bar{\gamma}_{1S_1R}^{-k_{12}+1} \bar{\gamma}_{2S_2R} \bar{\gamma}_{2S_2E}} \sum_{\bar{x}=1}^{N_3} \omega_{\bar{x}} H_3(y_{\bar{x}}), \tag{32}$$

where

$$H_3(y) = \frac{1}{(1 - k_2^2 y)^2} \exp\left\{-\frac{\gamma_0 + (\gamma_0 + 1)y}{\bar{\gamma}_{2S_2R} \{1 - \gamma_0 + (\gamma_0 + 1)y\}} - \frac{y}{\bar{\gamma}_{2S_2E} (1 - k_2^2 y)}\right\} \\ \times \left\{\Delta_{1S_1R} + \frac{(1 + k_1^2) [\gamma_0 + (\gamma_0 + 1)y]}{\bar{\gamma}_{2S_2R} \{1 - k_2^2 [\gamma_0 + (\gamma_0 + 1)y]\}}\right\}^{-k_{12}-1},$$

and N_3 being the number of the terms, $y_{\bar{x}} = \frac{H_3}{2} (x_{\bar{x}} + 1)$ represents the \bar{x} -th zero of Legendre polynomials, $\omega_{\bar{x}}$ represents the Gaussian weight, which can be seen in [40], and $H_3 = \min\left(\frac{1/k_2^2 - \gamma_0}{\gamma_0 + 1}, \frac{1}{k_2^2}\right)$.

$$\Pr(C_{S_{21}} < C_0) = 1 - \frac{H_4}{2} \sum_{k_{21}=0}^{m_{1S_1R}-1} \sum_{t=0}^{k_{12}} \frac{\alpha_{1S_1R} (1 - m_{1S_1R})_{k_{12}} (-\delta_{1S_1R})^{k_{12}}}{k_{12}! t! \bar{\gamma}_{1S_1R}^{-k_{12}+1} \Delta_{1S_1R}^{k_{12}-t+1} \bar{\gamma}_{RRE}} \sum_{\mu=1}^{N_4} \xi_{\mu} H_4(y_{\mu}), \tag{33}$$

where

$$H_4(y) = \frac{1}{(1 - k_R^2 y)^2} \left[\frac{\gamma_0 + (\gamma_0 + 1)y}{1 - k_R^2 \gamma_0 - k_R^2 (\gamma_0 + 1)y} \right]^t \exp\left[-\frac{\Delta_{1S_1R} \gamma_0 + \Delta_{1S_1R} (\gamma_0 + 1)y}{1 - k_R^2 \gamma_0 - k_R^2 (\gamma_0 + 1)y} - \frac{y}{\bar{\gamma}_{RRE} (1 - k_R^2 y)} \right]$$

and N_4 being the number of the terms, $y_{\mu} = \frac{H_4}{2} (x_{\mu} + 1)$ represents the μ -th zero of Legendre polynomials, ξ_{μ} denotes the Gaussian weight, which has the definition in [40], and $H_4 = \min\left(\frac{1/k_R^2 - \gamma_0}{\gamma_0 + 1}, \frac{1}{k_R^2}\right)$.

Then, by substituting Eqs. (30)–(33) into Eqs. (19)–(21), respectively. The closed-form expression for the SOP will be obtained, which is omitted here.

3.1.4 Asymptotic SOP

In what follows, the asymptotic behaviors for the SOP is obtained. When $\bar{\gamma}_L \rightarrow \infty$, $L \in \{2S_2R, 1S_1R, RRS_1, RRS_2\}$, then utilizing $\exp(-x) \approx 1 - x$ and $(A/x + B) \approx B$, Eqs. (30)–(33) will be obtained as

$$\Pr(C_{S_{11}} < C_0) = 1 \\ - \sum_{k_1=0}^{m_{1S_1R}-1} \sum_{t=0}^{k_1} \sum_{k_{11}=0}^{m_{S_1E}-1} \sum_{p=0}^t \binom{t}{p} \frac{(1 + k_2^2)^p p! \alpha_{S_1E} (1 - m_{S_1E})_{k_{11}} (-\delta_{S_1E})^{k_{11}} \alpha_{1S_1R} (1 - m_{1S_1R})_{k_1} (-\delta_{1S_1R})^{k_1}}{(k_{11}!)^2 \bar{\gamma}_{S_1E}^{-k_1+1} k_1! t! \bar{\gamma}_{1S_1R}^{-k_1+1} \Delta_{1S_1R}^{k_1-t+1} \bar{\gamma}_{2S_2R}} \\ \times \frac{H_1}{2} \sum_{l=1}^{N_1} w_l \left(\frac{[\gamma_0 + (\gamma_0 + 1)y_l]}{1 - k_1^2 [\gamma_0 + (\gamma_0 + 1)y_l]} \right)^t \left\{ 1 - \frac{\Delta_{1S_1R} [\gamma_0 + (\gamma_0 + 1)y_l]}{1 - k_1^2 [\gamma_0 + (\gamma_0 + 1)y_l]} \right\} \frac{y_l^{k_{11}}}{(1 - k_1^2 y_l)^{k_{11}+2}}, \tag{34}$$

$$\Pr(C_{S_{22}} < C_0) = 1 - \frac{H_2}{2\bar{\gamma}_{RRE}} \sum_{v=1}^{N_2} \frac{\omega_v}{(1 - k_R^2 y_v)^2} \left\{ 1 - \frac{\gamma_0 + (\gamma_0 + 1) y_v}{\bar{\gamma}_{RRS_2} \{1 - k_R^2 [\gamma_0 + (\gamma_0 + 1) y_v]\}} \right\}, \tag{35}$$

$$\Pr(C_{S_{12}} < C_0) = 1 - \frac{H_3}{2} \sum_{k_{12}=0}^{m_{1S_1R}-1} \frac{\alpha_{1S_1R} (1 - m_{1S_1R})_{k_{12}} (-\delta_{1S_1R})^{k_{12}}}{k_{12}! \bar{\gamma}_{1S_1R}^{-k_{12}+1} \bar{\gamma}_{2S_2R} \bar{\gamma}_{2S_2E}} \sum_{\bar{\lambda}=1}^{N_3} \frac{\omega_{\bar{\lambda}}}{(1 - k_2^2 y_{\bar{\lambda}})^2} \times \left[1 - \frac{\gamma_0 + (\gamma_0 + 1) y_{\bar{\lambda}}}{\bar{\gamma}_{2S_2R} [1 - \gamma_0 + (\gamma_0 + 1) y_{\bar{\lambda}}]} \right] \left\{ \Delta_{1S_1R} + \frac{(1 + k_1^2) [\gamma_0 + (\gamma_0 + 1) y_{\bar{\lambda}}]}{\bar{\gamma}_{2S_2R} \{1 - k_2^2 [\gamma_0 + (\gamma_0 + 1) y_{\bar{\lambda}}]\}} \right\}^{-k_{12}-1}, \tag{36}$$

and

$$\Pr(C_{S_{21}} < C_0) = 1 - \frac{H_4}{2} \sum_{k_{21}=0}^{m_{1S_1R}-1} \sum_{t=0}^{k_{12}} \frac{\alpha_{1S_1R} (1 - m_{1S_1R})_{k_{12}} (-\delta_{1S_1R})^{k_{12}}}{k_{12}! t! \bar{\lambda}_{1S_1R}^{-k_{12}+1} \Delta_{1S_1R}^{k_{12}-t+1} \bar{\gamma}_{RRE}} \sum_{\mu=1}^{N_4} \frac{\xi_{\mu}}{(1 - k_R^2 y_{\mu})^2} \times \left[\frac{\gamma_0 + (\gamma_0 + 1) y_{\mu}}{1 - k_R^2 \gamma_0 - k_R^2 (\gamma_0 + 1) y_{\mu}} \right]^t \left[1 - \frac{\Delta_{1S_1R} \gamma_0 + \Delta_{1S_1R} (\gamma_0 + 1) y_{\mu}}{1 - k_R^2 \gamma_0 - k_R^2 (\gamma_0 + 1) y_{\mu}} \right]. \tag{37}$$

Then by substituting Eqs. (34)–(37) into Eqs. (19)–(21), the asymptotic expression will be derived.

Then from the final asymptotic SOP expression, the secrecy diversity order and secrecy coding gain are respectively derived as

$$G_D = 1, \tag{38}$$

$$G_C = \sum_{k_1=0}^{m_{1S_1R}-1} \sum_{t=0}^{k_1} \sum_{k_{11}=0}^{m_{S_1E}-1} \sum_{p=0}^t \binom{t}{p} \frac{(1 + k_2^2)^p p! \alpha_{S_1E} (1 - m_{S_1E})_{k_{11}} (-\delta_{S_1E})^{k_{11}} \alpha_{1S_1R} (1 - m_{1S_1R})_{k_1} (-\delta_{1S_1R})^{k_1}}{(k_{11}!)^2 \bar{\gamma}_{S_1E}^{-k_{11}+1} k_1! t! (\alpha_{1S_1R} - \beta_{1S_1R})^{k_1-t+1}} \times \frac{H_1}{2} \sum_{l=1}^{N_1} w_l \left(\frac{[\gamma_0 + (\gamma_0 + 1) y_l]}{1 - k_1^2 [\gamma_0 + (\gamma_0 + 1) y_l]} \right)^t \left\{ 1 - \frac{(\alpha_{1S_1R} - \beta_{1S_1R}) [\gamma_0 + (\gamma_0 + 1) y_l]}{1 - k_1^2 [\gamma_0 + (\gamma_0 + 1) y_l]} \right\} + \frac{H_2}{2\bar{\gamma}_{RRE}} \sum_{v=1}^{N_2} \frac{\omega_v}{(1 - k_R^2 y_v)^2} \left\{ 1 - \frac{\gamma_0 + (\gamma_0 + 1) y_v}{\{1 - k_R^2 [\gamma_0 + (\gamma_0 + 1) y_v]\}} \right\} + \frac{H_3}{2} \sum_{k_{12}=0}^{m_{1S_1R}-1} \frac{\alpha_{1S_1R} (1 - m_{1S_1R})_{k_{12}} (-\delta_{1S_1R})^{k_{12}}}{k_{12}! \bar{\gamma}_{2S_2E}} \times \sum_{\bar{\lambda}=1}^{N_3} \frac{\omega_{\bar{\lambda}}}{(1 - k_2^2 y_{\bar{\lambda}})^2} \left[1 - \frac{\gamma_0 + (\gamma_0 + 1) y_{\bar{\lambda}}}{[1 - \gamma_0 + (\gamma_0 + 1) y_{\bar{\lambda}}]} \right] + \frac{H_4}{2} \sum_{k_{21}=0}^{m_{1S_1R}-1} \sum_{t=0}^{k_{12}} \frac{\alpha_{1S_1R} (1 - m_{1S_1R})_{k_{12}} (-\delta_{1S_1R})^{k_{12}}}{k_{12}! t! (\alpha_{1S_1R} - \beta_{1S_1R})^{k_{12}-t+1} \bar{\gamma}_{RRE}} \times \sum_{\mu=1}^{N_4} \frac{\xi_{\mu}}{(1 - k_R^2 y_{\mu})^2} \left[1 - \frac{(\alpha_{1S_1R} - \beta_{1S_1R}) \gamma_0 + (\alpha_{1S_1R} - \beta_{1S_1R}) (\gamma_0 + 1) y_{\mu}}{1 - k_R^2 \gamma_0 - k_R^2 (\gamma_0 + 1) y_{\mu}} \right]. \tag{39}$$

4 Numerical Results

During this part, some representative MC simulations are provided to prove the efficiency of the theoretical analysis. Through these results, the impacts of channel parameters are evaluated. Without loss of any generality, we set $\bar{\gamma}_{1S_1R} = \bar{\gamma}_{RRS_1} = \bar{\gamma}_{2S_2R} = \bar{\gamma}_{RRS_2} = \bar{\gamma}$, $\bar{\gamma}_{1S_1E} = \bar{\gamma}_{2S_2E} = \bar{\gamma}_{RRE} = \bar{\gamma}_E$ and $\delta_R^2 = \delta_{S_1}^2 = \delta_{S_2}^2 = \delta_E^2 = 1$, $k_1 = k_2 = k_R = k$. The system and channel parameters are shown in Table 2 [35] and Table 3 [7], respectively.

Table 2: System parameters

Parameters	Value
Satellite orbit	GEO
Frequency band	$f = 2$ GHz
3 dB angle	$\bar{\theta}_k = 0.8^\circ$
Maximal beam gain	$G_{max} = 48$ dB
The antenna gain	$G_{Re} = 4$ dB

Table 3: Channel parameters

Shadowing	m_V	b_V	Ω_V
Frequent heavy shadowing (FHS)	1	0.063	0.0007
Average shadowing (AS)	5	0.251	0.279
Infrequent light shadowing (ILS)	10	0.158	1.29

Fig. 2 examines the SOP vs. $\bar{\gamma}$ for different shadow fading and impairments' level with $\bar{\gamma}_E = 0$ dB and $\gamma_0 = 0$ dB. From Fig. 2, firstly, we can derive that the simulation results are tight across the theoretical analysis, which verify our analysis. In addition, in high SNR regime, the asymptotic results are nearly the same as the simulation results, which show the rightness of the analysis. Moreover, in this figure, it is very interesting that we find the SOP for AS scenario is lower than that of FHS, for the reason that when the channel suffers light fading, the system will have a better system performance. However, we find that the SOP for ILS scenario is the worst, which results in that when the channel is under ILS shadowing, the channel quality for eavesdropper is the best. In ILS scenario, the impact of channel quality on eavesdroppers is superior to that of legitimate users; thus the SOP is the highest. Finally, the lower hardware impairments' level leads to a lower SOP.

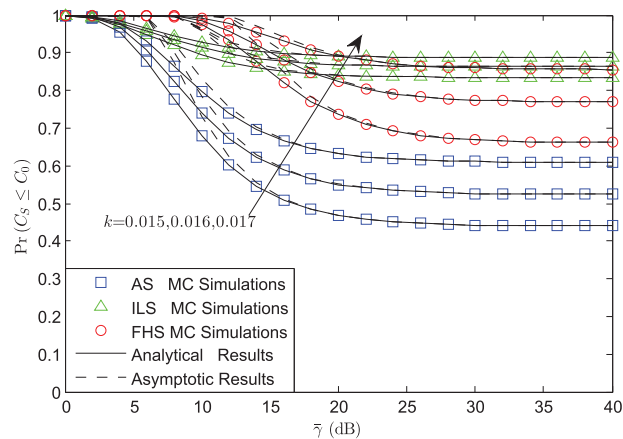
**Figure 2:** SOP vs. $\bar{\gamma}$ for different shadow fading and impairments' level with $\bar{\gamma}_E = 0$ dB and $\gamma_0 = 0$ dB

Fig. 3 represents the SOP vs. $\bar{\gamma}$ for different $\bar{\gamma}_E$ and impairments' level under AS scenario. From this figure, we can find that the SOP with lower $\bar{\gamma}_E$ will lead to a lower SOP for the quality of the eavesdroppers gets better. For the reason that a more powerful eavesdropper will derive this phenomenon.

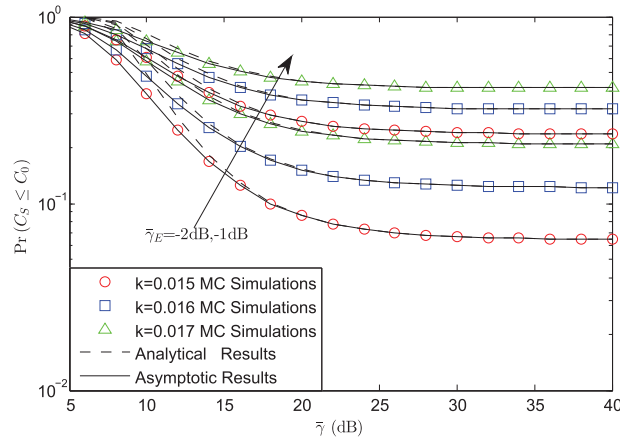


Figure 3: SOP vs. $\bar{\gamma}$ for different $\bar{\gamma}_E$ and impairments' level with $\gamma_0 = 0$ dB under AS scenario

Fig. 4 plots the SOP vs. γ_0 for different $\bar{\gamma}_E$ and impairments' level under AS scenario. It can be derived that, the SOP will be always 1, which means the system is in outage state all the time when the threshold grows to the special value. It can be also seen that this value just has the relationship with the HIs level. In addition, we find that a lower HIs level will bring a larger value. At last, it can be derived that the value for $\bar{\gamma}_E$ has no impact on this value.

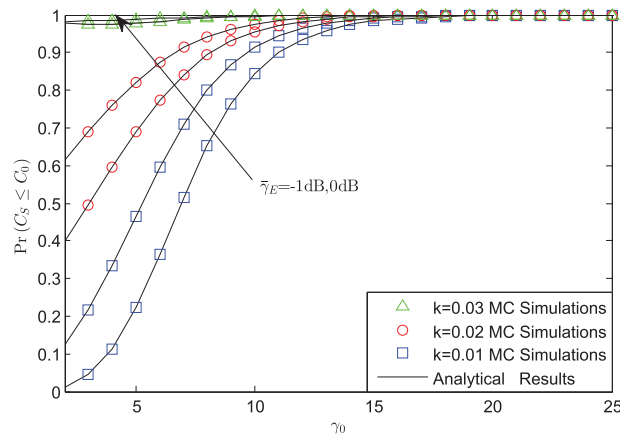


Figure 4: SOP vs. γ_0 for different $\bar{\gamma}_E$ and impairments' level under AS scenario

5 Conclusions

This paper investigated the SOP for an integrated satellite UAV relay network with HIs. Especially, the closed-form and asymptotic behaviors for the SOP were derived. Firstly, it was derived that the SOP would have worse performance with threshold being larger; Secondly, it was found that the SOP

would be larger with a larger $\bar{\gamma}_E$; Thirdly, it was seen that the HIs' level had a great impact on the SOP. A larger impairments' level brought a larger SOP; Finally, the channel fading also influenced the SOP.

Acknowledgement: The authors wish to express their appreciation to the reviewers for their helpful suggestions which greatly improved the presentation of this paper.

Funding Statement: This work is supported by the Natural Science Foundation of China under Grant No. 62001517.

Conflicts of Interest: The authors declare that they have no conflicts of interest to report regarding the present study.

References

1. Li, B., Fei, Z., Zhou, C., Zhang, Y. (2020). Physical layer security in space information networks: A survey. *IEEE Internet of Things Journal*, 69(5), 33–52. DOI 10.1109/JIOT.6488907.
2. Guo, K., Lin, M., Zhang, B., Zhu, W. P., Wang, J. B. et al. (2019). On the performance of LMS communication with hardware impairments and interference. *IEEE Transactions on Communications*, 67(2), 1490–1505. DOI 10.1109/TCOMM.2018.2878848.
3. Guo, K., Dong, C., An, K. (2022). NOMA-Based cognitive satellite terrestrial relay networks: Secrecy performance under channel estimation errors and hardware impairments. *IEEE Internet of Things Journal*, 9(18), 17334–17347. DOI 10.1109/JIOT.2022.3157673.
4. Liu, R., Guo, K., An, K., Zhu, S. (2022). NOMA-Based overlay cognitive integrated satellite-terrestrial networks with secondary networks selection. *IEEE Transactions on Vehicular Technology*, 71(2), 2187–2192. DOI 10.1109/TVT.2021.3122029.
5. Guo, K., An, K. (2022). On the performance of RIS-assisted integrated satellite-UAV-terrestrial networks with hardware impairments and interference. *IEEE Wireless Communications Letters*, 11(1), 131–135. DOI 10.1109/LWC.2021.3122189.
6. Kodheli, O., Lagunas, E., Maturo, N., Sharma, S. K., Shankar, B. et al. (2021). Satellite communications in the new space era: A survey and future challenges. *IEEE Communications Surveys Tutorials*, 23(1), 70–109. DOI 10.1109/COMST.9739.
7. Guo, K., Lin, M., Zhang, B., Wang, J. B., Wu, Y. et al. (2020). Performance analysis of hybrid satellite-terrestrial cooperative networks with relay selection. *IEEE Transactions on Vehicular Technology*, 69(8), 9053–9067. DOI 10.1109/TVT.25.
8. Guo, K., An, K., Zhang, B., Huang, Y., Guo, D. et al. (2019). On the performance of the uplink satellite multi-terrestrial relay networks with hardware impairments and interference. *IEEE Systems Journal*, 13(3), 2297–2308. DOI 10.1109/JSYST.4267003.
9. An, K., Lin, M., Zhu, W. P., Huang, Y., Zheng, G. (2016). Outage performance of cognitive hybrid satellite-terrestrial networks with interference constraint. *IEEE Transactions on Vehicular Technology*, 65(11), 9397–9404. DOI 10.1109/TVT.2016.2519893.
10. Sharma, P. K., Upabhat, P. K., da Costa, D. B., Bithas, P. S., Kanatas, A. G. (2017). Performance analysis of overlay spectrum sharing in hybrid satellite-terrestrial systems with secondary network selection. *IEEE Transactions on Wireless Communications*, 16(10), 6586–6601. DOI 10.1109/TWC.2017.2725950.
11. Upadhyay, P. K., Sharma, P. K. (2016). Max-max user-relay selection scheme in multiuser and multi-relay hybrid satellite-terrestrial relay systems. *IEEE Communications Letters*, 20(2), 268–271. DOI 10.1109/LCOMM.2015.2502599.

12. Zhao, Y., Xie, L., Chen, H., Wang, K. (2017). Ergodic channel capacity analysis of downlink in the hybrid satellite-terrestrial cooperative system. *Wireless Personal Communications*, 96(3), 3799–3815. DOI 10.1007/s11277-017-4207-2.
13. An, K., Lin, M., Liang, T. (2015). On the performance of multiuser hybrid satellite-terrestrial relay networks with opportunistic scheduling. *IEEE Communications Letters*, 19(10), 1722–1725. DOI 10.1109/LCOMM.2015.2466535.
14. Tang, X., An, K., Guo, K., Wang, S., Wang, X. et al. (2019). On the performance of two-way multiple relay non-orthogonal multiple access based networks with hardware impairments. *IEEE Access*, 7, 128896–128909. DOI 10.1109/Access.6287639.
15. Guo, K., Zhang, B., Huang, Y., Guo, D. (2017). Performance analysis of two-way satellite terrestrial relay networks with hardware impairments. *IEEE Wireless Communications Letters*, 6(4), 430–433. DOI 10.1109/LWC.2017.2700797.
16. Zeng, W., Zhang, J., Ng, D., Ai, B., Zhong, Z. (2019). Two-way hybrid terrestrial-satellite relaying systems: Performance analysis and relay selection. *IEEE Transactions on Vehicular Technology*, 68(7), 7011–7023. DOI 10.1109/TVT.2019.2916992.
17. Guo, K., An, K., Zhang, B., Guo, D. (2018). Performance analysis of two-way satellite multi-terrestrial relay networks with hardware impairments. *Sensors*, 18(5), 1–19. DOI 10.3390/s18051574.
18. Guo, K., An, K., Zhang, B., Huang, Y., Tang, X. et al. (2020). Physical layer security for multiuser satellite communication systems with threshold-based scheduling scheme. *IEEE Transactions on Vehicular Technology*, 69(5), 5129–5141. DOI 10.1109/TVT.2020.2979496.
19. Li, B., Fei, Z., Chu, Z., Zhou, F., Wong, K. K. et al. (2018). Robust chance-constrained secure transmission for cognitive satellite-terrestrial networks. *IEEE Transactions on Vehicular Technology*, 67(5), 4208–4219. DOI 10.1109/TVT.2018.2791859.
20. Li, B., Fei, Z., Xu, X., Chu, Z. (2018). Resource allocations for secure cognitive satellite-terrestrial networks. *IEEE Wireless Communications Letters*, 7(1), 78–81. DOI 10.1109/LWC.2017.2755014.
21. Lin, Z., Lin, M., Champagne, B., Zhu, W. P., Naofal, A. D. (2021). Secrecy-energy efficient hybrid beamforming for satellite-terrestrial integrated networks. *IEEE Transactions on Communications*, 69(9), 6345–6360. DOI 10.1109/TCOMM.2021.3088898.
22. An, K., Lin, M., Ouyang, J., Zhu, W. P. (2016). Secure transmission in cognitive satellite terrestrial networks. *IEEE Journal on Selected Areas in Communications*, 34(11), 3025–3037. DOI 10.1109/JSAC.2016.2615261.
23. Li, X., Huang, M., Liu, Y., Menon, V. B., Paul, A. et al. (2021). I/Q imbalance aware nonlinear wireless-powered relaying of B5G networks: Security and reliability analysis. *IEEE Transactions Network Science and Engineering*, 8(4), 2995–3008. DOI 10.1109/TNSE.2020.3020950.
24. Li, X., Zheng, Y., Alshehri, M. D., Hai, L., Balasubramanian, V. et al. (2021). Cognitive AmBC-NOMA IoV-MTS networks with IQI: Reliability and security analysis. *IEEE Transactions Intelligent Transportation Systems*. DOI 10.1109/TITS.2021.3113995.
25. Li, X., Li, J., Liu, Y., Ding, Z., Nallanathan, A. (2020). Residual transceiver hardware impairments on cooperative NOMA networks. *IEEE Transactions on Wireless Communications*, 19(1), 680–695. DOI 10.1109/TWC.7693.
26. Bjornson, E., Matthaiou, M., Debbah, M. (2013). A new look at dual-hop relaying: Performance limits with hardware impairments. *IEEE Transactions on Communications*, 61(11), 4512–4525. DOI 10.1109/TCOMM.2013.100913.130282.
27. Zhang, J., Dai, L., Zhang, X., Bjornson, E., Wang, Z. (2016). Achievable rate of rician large-scale MIMO channels with transceiver hardware impairments. *IEEE Transactions on Vehicular Technology*, 65(10), 8800–8806. DOI 10.1109/TVT.2015.2504428.
28. Budimir, D., Neskovic, N., Cabarkapa, M. (2016). Hardware impairments impact on fixed-gain AF relaying performance in Nakagami- m fading. *Electronics Letters*, 52(2), 121–122. DOI 10.1049/el.2015.3378.

29. Duy, T. T., Duong, T. Q., da Costa, D. B., Bao, V. N. Q., Elkashlan, M. (2015). Proactive relay selection with joint impact of hardware impairments and co-channel interference. *IEEE Transactions on Communications*, 63(5), 1594–1606. DOI 10.1109/TCOMM.2015.2396517.
30. Deng, C., Liu, M., Li, X., Liu, Y. (2021). Residual transceiver hardware impairments on cooperative NOMA networks. *IEEE Systems Journal*, 19(1), 680–695.
31. Li, X., Zhao, M., Zeng, M., Mumtaz, S., Menon, V. G. et al. (2021). Hardware impaired ambient backscatter NOMA system: Reliability and security. *IEEE Transactions on Communications*, 69(4), 2723–2736. DOI 10.1109/TCOMM.2021.3050503.
32. Guo, K., Lin, M., Zhang, B., Ouyang, J., Zhu, W. P. (2018). Secrecy performance of satellite wiretap channels with multi-user opportunistic scheduling. *IEEE Wireless Communications Letters*, 7(6), 1054–1057. DOI 10.1109/LWC.2018.2859385.
33. Guo, K., An, K., Zhang, B., Huang, Y., Guo, D. (2018). Physical layer security for hybrid satellite terrestrial relay networks with joint relay selection and user scheduling. *IEEE Access*, 6, 55815–55827. DOI 10.1109/ACCESS.2018.2872718.
34. Arnau, J., Christopoulos, D., Chatzinotas, S., Mosquera, C., Ottersten, B. (2014). Performance of the multi-beam satellite return link with correlated rain attenuation. *IEEE Transactions on Wireless Communications*, 13(11), 6286–6299. DOI 10.1109/TWC.2014.2329682.
35. Guo, K., An, K., Zhou, F., Theodoros, A. T., Zheng, G. et al. (2021). On the secrecy performance of NOMA-based integrated satellite multipleterrestrial relay networks with hardware impairments. *IEEE Transactions on Vehicular Technology*, 70(4), 3661–3676. DOI 10.1109/TVT.2021.3068062.
36. Abdi, A., Lau, W. C., Alouini, M. S., Kaveh, M. (2003). A new simple model for land mobile satellite channels: First-and second-order statistics. *IEEE Transactions on Wireless Communications*, 2(3), 519–528. DOI 10.1109/TWC.2003.811182.
37. Loo, C. (1985). A statistical model for a land mobile satellite link. *IEEE Transactions on Vehicular Technology*, 34(3), 122–127.
38. Loo, C., Butterworth, J. S. (1988). Land mobile satellite channel measurements and modeling. *Proceeding of the IEEE*, 86, 1442–1463.
39. Gradshteyn, I. S., Ryzhik, I. M. (2007). *Table of integrals, series and products*. Boston, USA: Academic Press.
40. Abramowitz, M., Stegun, I. A. (1972). *Handbook of mathematical functions with formulas, graphs, and mathematical tables*. Florida, USA: CRC Press.